Influence of interface voltage on charge build-up under high voltage

Lin Zheng, Stéphane Holé

Influence of interface voltage on charge build-up under high voltage

Lin Zheng and Stéphane Holé

Laboratoire de Physique et d'Étude des Matériaux (UMR 8213)
Sorbonne University – ESPCI Paris, PSL University – CNRS
10, rue Vauquelin – 75005 Paris – France

Corresponding author: lin.zheng@espci.fr

November 25, 2024

Abstract

The interface voltage appearing when two materials are brought into contact was measured with a high sensitive pressure-wave-propagation measurement setup in various low density and high density polyethylene samples coated either with aluminum or gold electrodes. The samples were then tested under high voltage (40 kV/mm) for 24 h to assess the correlation between interface voltage and charge injection at 22 °C. Aluminum electrodes induce a positive interface voltage toward the insulator favoring electron injection at the cathode while gold electrodes induce a negative interface voltage toward the insulator favoring hole injection at the anode. After the injections due to interface voltage, charges diffuse more easily in low density polyethylene that triggers a subsequent injection due to heterocharges buildup.

1 Introduction

Space charge is an important factor affecting the efficiency of insulators as the electric field they produce superimposes to the applied one, leading to bias [1], or even to breakdown [2]. Charges that accumulate in insulating materials under high voltage originate either from the insulator itself, through dissociation and molecular migration, or from the injection of charges through interfaces with adjacent materials, most often the electrodes subjected to voltage [3, 4]. When two materials with different work functions come into contact, charges of the highest energy level on one side are pushed to the other side generating in turn a dipole at the interface and thus an interface voltage (or contact potential) is formed [5]. At equilibrium the Fermi levels are equal in both materials [6].

In the case of semi-conductors, it is well known that interface voltages change the energy level shape [5, 7], the bands being bent on a distance proportional to the Debye length [6, 7]. As Debye length is inversely proportional to the square root of the mobile carrier density, it tends to infinity in the case of perfect insulators. As a consequence, energy levels are often considered flat with a slope corresponding only to the voltage applied to the insulator [7]. In fact, interface dipoles have been directly detected

at metal/insulator interfaces [8], some exhibiting a clear bipolar shape indicating a variation of the potential on a much smaller scale than expected. This would result in the energy band bending and hence in a higher barrier lowering for the Schottky injection law [4]. Therefore, the interface voltage observed at metal/insulator interfaces may greatly impact charge injection in insulators subjected to high voltage.

In order to investigate the correlation between intrinsic interface voltage and charge build-up in insulators under high voltage, the pressure-wave-propagation (PWP) method was chosen to perform non-destructive space charge distribution measurements [9]. The PWP method is a direct and non-destructive charge distribution measurement method based on an elasto-electric coupling [10]. The interface dipoles due to the contact potential can be detected [8] by using a high-sensitive set-up [11]. Compared to the thermal methods [11], PWP signals are easier to analyze as a post processing is not mandatory. Compared to the pulsed electro-acoustic (PEA) method [12], PWP method does not induce additional signals at the interfaces that mask the effect of interest. Indeed, the voltage pulse excitation used in PEA method induces charges on the electrodes at the origin of a quadratic signal at the interface which become very important when small signals are to be detected [13].

In this present study, various low density and high density polyethylene samples were tested as they are widely used in power transmission and distribution systems [14]. The main advantage of polyethylene lies in its electrical properties, such as high breakdown field, low dielectric loss and very low electrical conductivity [15, 16], all this at low price. In the first section, samples, set-up, measurement protocol and calibration procedure are presented. Results are shown and discussed in the second section before conclusion.

2 Samples and experimental protocols

2.1 Samples

Two kinds of polyethylene samples were studied, low density polyethylene (LDPE) and high density polyethylene (HDPE). All samples are 1-mm thick and were cut out from the same polymer sheet to limit dispersion in the results. Samples were coated under vacuum on both sides by aluminum or by gold. Samples prepared for interface voltage measurements are 3-cm diameter and electrodes are 2-cm diameter whereas samples prepared for high voltage measurements are 20-cm diameter and electrodes are 5-cm diameter. All samples were cured 1 week at 60 °C under short-circuit to remove the static charges.

2.2 Measurement set-up

The principle of the PWP method is presented in Figure 1. Pressure pulses are generated by a piezoelectric actuator [17]. During the propagation in the sample at the velocity of sound, each pressure pulse displaces charges and thus produces a measurable current in the circuit connecting the electrodes. This current is an image of the charge distribution where charge position can be deduced from the time of appearance in the signal multiplied by the velocity of sound. The piezoelectric generator is made of a 15 mm-diameter 0.2 mm-thick Pz24 piezoelectric ceramic from Meggitt stuck by epoxy resin with a 3-cm-long brass backing on one side and an aluminum wave-guide on the other side. The wave-guide

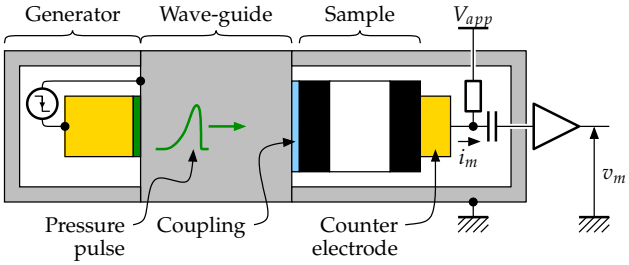

Figure 1: Principle of the pressure-wave-propagation method.

is 2-cm long for the contact potential measurement setup and 3-cm long for the high voltage measurement setup. This structure has a derivative response, thus generates a pressure pulse by applying a step voltage [17]. Pressure pulses with an amplitude greater than 1-MPa were generated every 20 ms [18]. By using averaging, it is possible to detect electric fields as low as 1 V/mm within a 1-mm thick polyethylene samples.

As high voltage insulators are often coated with carbon loaded polymer electrodes to smooth electric field around metallic parts, the samples were squeezed with carbon loaded Ethylene Vinyl Acetate (EVA) polymer electrodes on both sides between the Al wave-guide and a brass counter electrode, which exerted about 0.5-bar static pressure. Silicone oil is used as a coupling medium between each layers to ensure a good acoustical contact with the wave-guide. Notice that silicone oil is often used in high voltage applications to avoid gaseous region between materials [19]. The signal was amplified by a 66-dB HCA-10M-100K FEMTO amplifier, then acquired and averaged by a MSO44 Tektronix scope. A picture of the high voltage setup is shown in Figure 2.

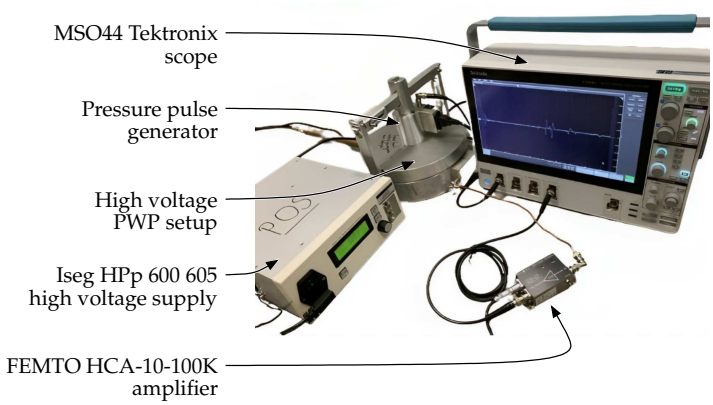

Figure 2: Picture of the PWP setup used for high voltage measurements. It consists of a PWP set-up connected to a high-voltage generator, an amplifier and an oscilloscope.

2.3 Measurement protocol

The flowchart in Figure 3 illustrates the sample preparation and measurement protocol for the high voltage samples. Similar protocol was used for the contact potential measurements [8]. The samples were prepared and then cured at 60 °C under short-circuit for 7 days to release all the residual charges due to sample preparation and finally placed in the PWP setup. The two first measurements were performed under short-circuit, one with an amplifier (red dot in Figure 4) the other without. Before applying the voltage, a simple way to ensure that no residual charge remains in the sample is to calculate

the electric field from the two first measured signals. If the electric field is zero beside interface charge distributions, the protocol can continue; otherwise the sample must be cured for a longer time. The voltage was switched on and the third measurement was carried out under 40 kV.

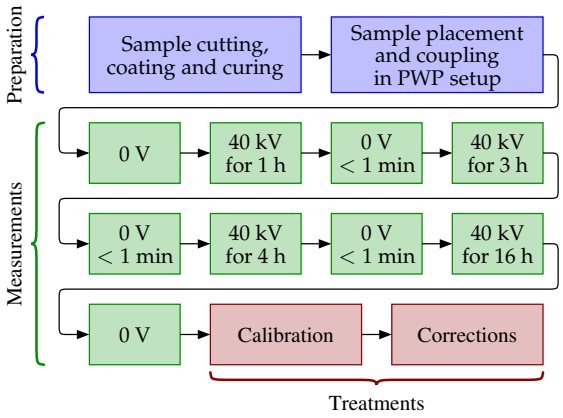

Figure 3: Flowchart of the measurement protocol from the sample preparation to the signal calibration.

After that, space charges were measured at various times of the voltage application according to the protocol sketched in Figure 4: after 1 h, 4 h, 8 h and 24 h. Each time, a series of measurements was taken. A measurement was carried out under voltage, then the voltage was switched off for less than 1 min, and two measurements were performed under short-circuit, one without amplifier and one with amplifier (red dots in Figure 4), then the voltage was switched on again and a last measurement was carried out without amplifier. In total, 18 measurements were performed each being the average of 1000 acquisitions.

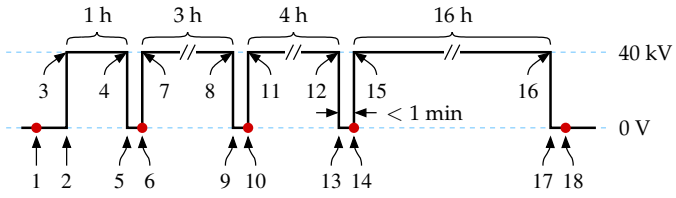

Figure 4: Measurement protocol for the samples under high voltage. All 18 measurements were performed under 40 kV or short-circuit conditions over a 24-hour period. Red dots indicate measurements with an amplifier.

The short-circuit periods lasted less than 1 min to prevent charge previously injected under voltage from relaxation. These short-circuit periods are interesting for charge injection detection since capacitive charges caused by high voltage no longer mix in the signal with injected charges. Indeed under high voltage (see Figure 5a), induced charges and injected charges produce a signal of same polarity thus difficult to discriminate since the signal is a pulse with or without injection. On the contrary, injected charges and induced charges have opposite polarities under short-circuit (see Figure 5b), which leads to a clear detection. Also, the protocol allows the calibration to be evaluated at any time by a simple subtraction between the last measurement under voltage with the first following measurement under short-circuit. This further ensure that everything was going correctly without drift.

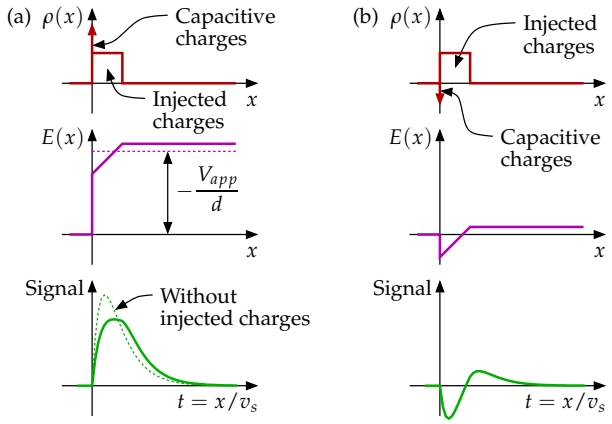

Figure 5: Clear injection charge detection. (a) Under voltage V_{app}, injected charges and capacitive charges are of the same polarity. The signal remains a pulse with or without injection. (b) Under short-circuit, injected charges and capacitive charges are of opposite polarity, thus easy to distinguish. In this sketch, charge injection amplitude has been overplayed for sake of clarity. Charge density is ρ, electric field is E, d is insulator thickness, x is position, t is time and v_s is sound velocity.

2.4 Calibration and analysis technique

The measured current $i_m(t)$ is expressed as [20]

$$i_m(t) = -C_0 \int (1 - a/\varepsilon) E(x) \frac{\partial S(x,t)}{\partial t} \, \mathrm{d}x, \tag{1}$$

where C_0 is the capacitance of the sample, a its electrostrictive coefficient, ε its permittivity, x is the position in depth, t is the time, $S(x,t)$ is the strain due to the pressure pulse and $E(x)$ is the electric field distribution. Assuming that the insulating polymer is uniform, a and ε can get out of the integral. Moreover, since $\partial S/\partial t = \partial V/\partial x$ with $V(x,t)$ the particle velocity, using Gauss-Maxwell equation to introduce charge density $\rho(x)$ and after an integration by parts, it comes

$$i_m(t) = \frac{C_0}{\varepsilon}(1 - a/\varepsilon) \int \rho(x) V(x,t) \, \mathrm{d}x. \tag{2}$$

This expression simply demonstrates that the measured current is due to all charges displaced at particle velocity $V(x,t)$ in the sample due to the pressure wave. The calibration consists in submitting the insulator to a known electrical field to deduce the conversion coefficient. One way is to use the surface charge induced on the electrodes when the sample is under voltage (see Figure 6). For a surface charge distribution $\rho(x) = \sigma\delta(x)$ with $\delta(x)$ the Dirac function, σ is the surface charge density defined as $\sigma = -\varepsilon V_{app}/d$ where V_{app} is the applied voltage and d is the sample thickness. In this specific situation, the signal can be called the calibration current $i_{cal}(t)$, which is at the first interface

$$i_{cal}(t) = -C_0(1 - a/\varepsilon)\frac{V_{app}}{d} V(x = 0, t). \tag{3}$$

Due to the property of propagation

$$\int V(t - x/v_s)\mathrm{d}t = -v_s \int V(t - x/v_s)\mathrm{d}x, \tag{4}$$

where v_s is the speed of sound (to be not confused with particle velocity) hence the integration over time of $i_{cal}(t)$ leads to

$$\begin{aligned} \int i_{cal}(t)\,\mathrm{d}t = & \quad -C_0(1-a/\varepsilon)\frac{V_{app}}{d}\int V(t-x/v_s)\,\mathrm{d}t \\ = & \quad C_0(1-a/\varepsilon)\frac{V_{app}}{dv_s}\int V(t-x/v_s)\,\mathrm{d}x. \end{aligned} \tag{5}$$

The amplitude of the integral over time of $i_{cal}(t)$ (see A in Figure 6) gives all the required information on the measurement setup. Dividing any further measured signals (obtained in the same conditions) with this amplitude links the charge distribution to known parameters as:

$$\begin{aligned} \frac{i_m(t)}{A} = & \quad \frac{(C_0/\varepsilon)(1-a/\varepsilon)\int \rho(x)V(x,t)\,\mathrm{d}x}{C_0(1-a/\varepsilon)V_{app}/(v_s d)\int V(x,t)\,\mathrm{d}x} \\ = & \quad \frac{v_s d}{\varepsilon V_{app}} < \rho > (x = v_s t). \end{aligned} \tag{6}$$

Therefore, the charge density at position x is found in the signal at time $t = x/v_s$ and its average amplitude on the extent of the pressure pulse can be obtained by

$$< \rho > (x = v_s t) = \frac{\varepsilon V_{app}}{v_s d}\frac{i_m(t)}{A}. \tag{7}$$

Notice that sound speed v_s can be easily determined by the ratio of the sample thickness d and the transit time of the pressure pulse in the sample (see Δt in Figure 6).

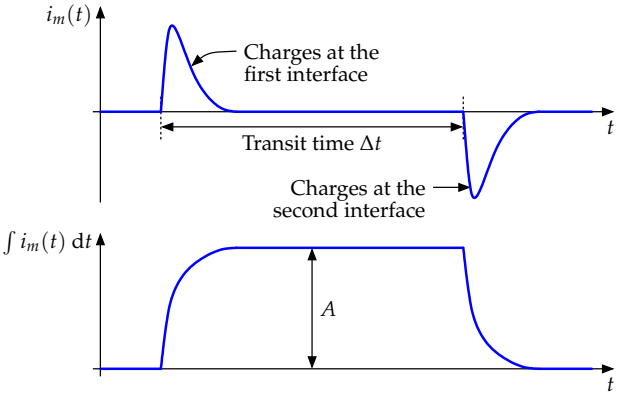

Figure 6: Schematic diagram of the measured signal $i_m(t)$ and its integral when charges only come from an applied voltage. A is the amplitude of the first peak integral.

In presence of interface dipoles, the signal $i_\pi(t)$ exhibits a bipolar peak at the interface [8] since a dipole contains two opposite charges. In that case, the interface voltage or contact potential v_π is obtained by a double integral over time of the bipolar signal at the interface with

$$v_\pi = \frac{v_s V_{app}}{d}\frac{\iint i_\pi(t)\mathrm{d}t^2}{A}. \tag{8}$$

Notice that v_s/d corresponds directly to the transit time Δt of the pressure pulse in the sample (see Figure 6). It is relatively simple to convert interface voltage v_π to interface dipole π since they are connected by $v_\pi = \pi/\varepsilon$.

3 Results

3.1 Interface voltage

Measurements with LDPE samples under low voltages have been combined following the procedure described in [8] in order to obtain calibrated interface dipoles. The scale is in coulomb per cubic meter, which is convenient for charge density, and in volt per square microsecond, which is convenient for a direct interface voltage estimation from the double integration of the signal over time following (8), the correction coefficient $v_s V_{app}/dA$ being 1.71×10^5 $(\mu s)^{-2}$.

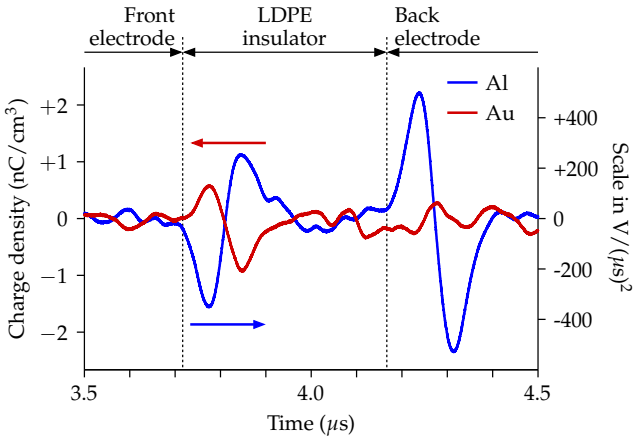

Figure 7: Calibrated combined signals of interface dipole at the interface of LDPE samples. Samples were coated with gold or aluminum electrodes, and coupled with 1 mm-thick carbon-loaded Ethylene Vinyl Acetate polymer (EVA) through silicone oil and tested in the PWP setup at room temperature. The polarity of the contact potential at the first interface is indicated by an arrow.

Figure 7 shows the influence of the coating. A first bipolar signal appears at 3.72 μs which corresponds to the time the pressure takes to cross the aluminum wave-guide and the carbon-loaded electrode. This bipolar signal is the image of the interface dipole at the first interface of the insulator (front electrode). The interface voltages estimated from the double integration over time according to (8) are -0.72 V and $+2.09$ V for gold and aluminum electrodes respectively. An approximate interface voltage can be directly calculated from the displayed curves with

$$v_\pi \approx -A_1 \tau_1 \, (\tau_1 + \tau_2), \tag{9}$$

where A_1 is the algebraic amplitude of the first dipole peak in V/$(\mu s)^2$ and τ_1 and τ_2 are respectively the duration at mid amplitude of the two dipole peaks in μs. One finds -0.63 V for gold and $+2.3$ V for aluminum with this approximation. The pressure pulse then propagates through the 1 mm-thick sample and generates a second bipolar signal at about 4.16 μs in LDPE when it arrives at the second interface of the insulator (back electrode). As partial reflections could make interpretation more tricky at the back electrode, only the front electrode signal is analyzed in this study. Notice however that dipoles are oriented to the same direction with respect to the insulator for both interfaces, which is logical since the structure is quasi symmetrical.

The Al-coated sample presents a positive interface voltage at the first interface which means that the positive charge is inside the insulator whereas the negative charge is held by the electrode. Therefore it can be said that the potential inside the insulator is positive compared to the one in the electrode,

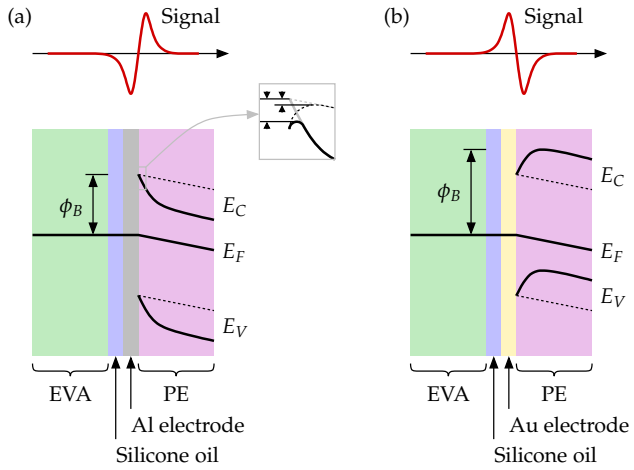

Figure 8: Energy level bending at the cathode of the insulator due to the interface voltage. Dotted lines correspond to infinite Debye length insulators whereas solid lines correspond to actual situation. (a) Case of a dipole directed from the electrode to the insulator (case of aluminum). The interface electric field is increased thus Schottky barrier $\phi_B - \beta\sqrt{E}$ is reduced as well as barrier thickness (see inset). (b) Case of a dipole directed from the insulator to the electrode (case of gold). The overall barrier ϕ_B is increased.

and thus the energy levels are bent downward for the insulator. This is illustrated in Figure 8a. As a consequence of the conduction band bending, the interface electric field E is larger than the one applied which reduces the Schottky barrier $\phi_B - \beta\sqrt{E}$ [4] as well as the barrier thickness. This promotes in turn electron injection. On the contrary, the bending takes the insulator valence band away from the Fermi level, reducing in turn electron extraction (hole injection). As to gold coating, the interface voltage is negative. The potential inside the insulator is hence lower than the one in the electrode, thus bending the energy band of the insulator upward as sketched in Figure 8b. In this case, electron injection should be impaired since the conduction band gets farther from the Fermi level whereas hole injection is promoted since the Schottky barrier is reduced. Notice that the observed interface dipole is the result of the overall interface voltage which takes into account EVA electrode, silicone oil, deposited electrode and PE. Spatial resolution is not sufficient to distinguish between each contribution.

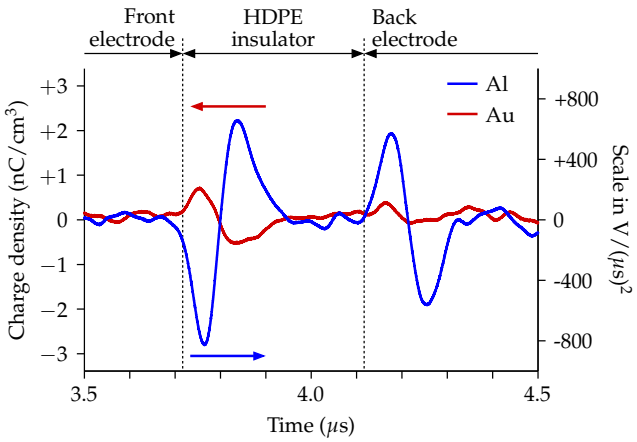

Figure 9: Calibrated combined signals of interface dipole at the interface of HDPE samples. Samples are coated with gold or aluminum electrodes, and coupled with 1 mm-thick carbon-loaded Ethylene Vinyl Acetate polymer (EVA) through silicone oil and tested in the PWP setup at room temperature. The polarity of the contact potential at the first interface is indicated by an arrow.

Figure 9 illustrates the calibrated interface dipoles for HDPE samples. The same protocol as the one of LDPE was applied. Though the first interface is detected at the same time, the second interface is detected slightly before than in LDPE since sound speed is slightly larger in HDPE than in LDPE. The double integration over time gives the interface voltages of -0.81 V and $+4.22$ V for gold and aluminum electrodes respectively.

For aluminum coating, the interface voltage is positive. This configuration causes the insulator conduction band to get closer to the electrode Fermi level, resulting in an easier electron injection at the cathode (see Figure 8a). For gold coating, the interface voltage is negative thus increasing the insulator valence band closer to the electrode Fermi level, which promotes hole injection at the anode (see Figure 8b).

In both kinds of material, aluminum coating should promote electron injection due to a positive intrinsic interface voltage toward the insulator whereas gold coating should promote hole injection due to a negative intrinsic interface voltage toward the insulator.

3.2 LDPE samples under high voltage

LDPE samples were tested at 22 °C under 40 kV for 24 h in agreement with the procedure described in Figure 4. The high voltage was thus momentarily deactivated to carry out measurements under short-circuit in order to better detect charge injection as already discussed in Section 2.3. As the aluminum wave-guide is 30-mm thick for high voltage setup, the pressure pulse takes 4.71 μs to propagate through it and additional 0.52 μs are required to cross the carbon-loaded electrode and reach the front interface of the insulator. The back electrode interface is reached 0.45 μs latter. These two interfaces are materialized by dotted lines. Under voltage, the front electrode was the cathode and the back electrode was the anode.

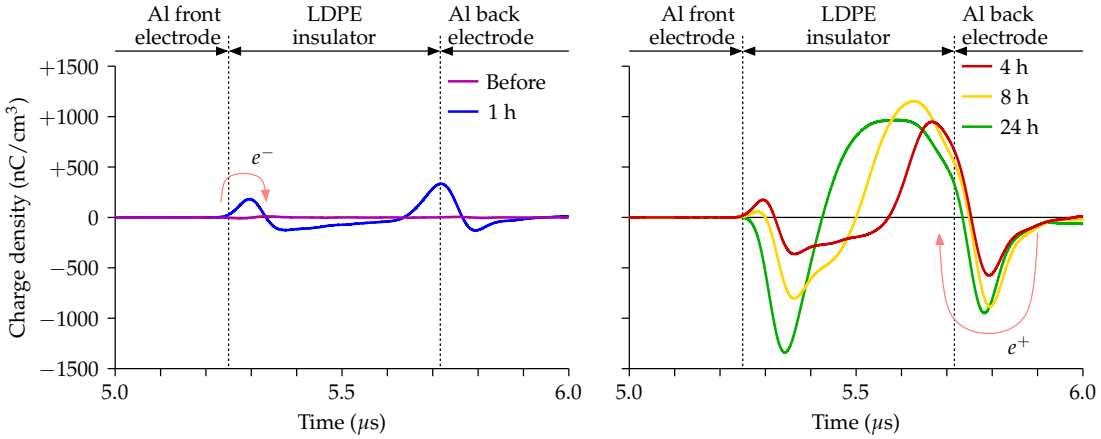

Figure 10: Signals of charge injection in LDPE samples measured under short-circuit for various durations under 40 kV at 22 °C. Samples are coated with aluminum electrodes and coupled with 1 mm-thick carbon-loaded polymer (EVA) through silicone oil and tested in the PWP setup. Dotted lines indicate when the pressure pulse began to cross an interface, the direction of movement of electrons and holes is illustrated by the pink arrow.

With aluminum electrodes, Figure 10 shows on top the charge distribution after 1 h. Positive charges are present at the front and back electrodes whereas negative charges spread almost evenly across the insulator. The positive peaks on the electrodes correspond to charges induced by the negative charges in the bulk of the insulator. It can be said that negative charges have been injected at the cathode and

diffused rapidly (within 1 h) through the whole sample structure. This is in accordance with the interface voltage orientation resulting in the lowering of the insulator conduction band. On a larger time scale, the increase of the electric field at the anode due to charge migration triggered an injection of holes that slowly diffused, and gradually penetrated deeper into the sample with time. At the end, two regions are clearly identified with negative charges close to the cathode and positive charges close to the anode, though positive charges dominate the sample at the end of the procedure (Figure 10, bottom).

With gold electrodes (Figure 11, top), there was little charge injection at the cathode that can be detected in the bulk. The quasi absence of the positive induced charges on the front electrode shows that positive charges injected from the anode induced a similar quantity of charges on the front electrode but of opposite polarity. This indicates that positive charges dominate till the beginning which is compatible with a hole injection expected due to the interface voltage that increased the insulator valence band. This hole injection at the anode continued and positive charges dominate the sample at the end of the procedure (Figure 11, bottom).

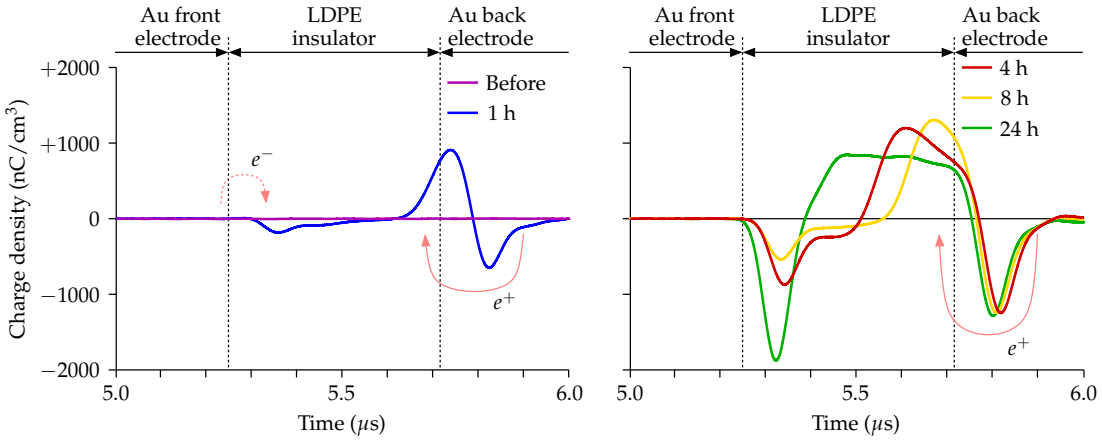

Figure 11: Signals of charge injection in LDPE samples measured under short-circuit for various durations under 40 kV at 22 °C. Samples are coated with gold electrodes, and coupled with 1 mm-thick carbon-loaded polymer (EVA) through silicone oil and tested in the PWP setup. Dotted lines indicate when the pressure pulse began to cross an interface, the direction of movement of electrons and holes is illustrated by the pink arrow.

In all cases, the interface voltage triggered the injection, electron injection at the cathode with aluminum coating and hole injection at the anode with gold coating. These injected charges rapidly diffused inside the sample increasing the electric field at the other electrode. As a consequence, this triggered a subsequent charge injection, not due to interface voltage in that case but to heterocharges. Finally, two step injection can be assumed, the first step depending on interface voltage, and the second step depending on the build up of heterocharges. These high voltage measurement results are similar to the ones obtained by G. Chen *et al.* [21], the interface voltage measured here explain the dynamics.

3.3 HDPE samples under high voltage

Similarly, HDPE samples were tested at 22 °C under 40 kV for 24 h. The pressure pulse arrived at the front interface at the same time as LDPE sample (5.23 μs) and reached the back interface 0.41 μs latter due to a slightly larger sound speed in HDPE than in LDPE. These two interfaces are materialized by dotted lines. Under voltage, the front electrode was the cathode and the back electrode was the anode.

When coated with aluminum electrodes, as shown in Figure 12, a strong bipolar peak is observed at front electrode, due to charge injection at the cathode and reached rapidly their position inside the sample without deeply diffusing. Indeed, though the amplitude of the signal increases progressively with time meaning more charges are injected, the shape of the distribution only little evolves. At the back interface, the signal exhibits an unipolar peak corresponding to the induced charges on the electrode due to the negative charges in the bulk. No charge was injected at the anode. Such a situation suggests that the Fermi level of the electrode is closer to the insulator conduction band than to the insulator valence band as anticipated by interface voltage measurements.

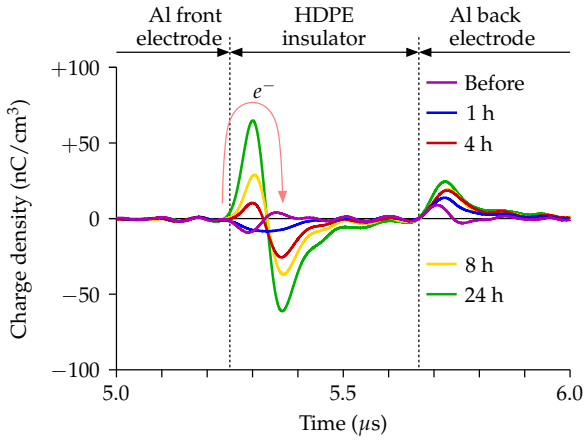

Figure 12: Signals of charge injection in HDPE samples measured under short-circuit for various durations under 40 kV at 22 °C. Samples are coated with aluminum electrodes, and coupled with 1 mm-thick carbon-loaded polymer (EVA) through silicone oil and tested in the PWP setup. Dotted lines indicate when the pressure pulse begains to cross an interface, the direction of movement of electrons and holes is illustrated by the pink arrow.

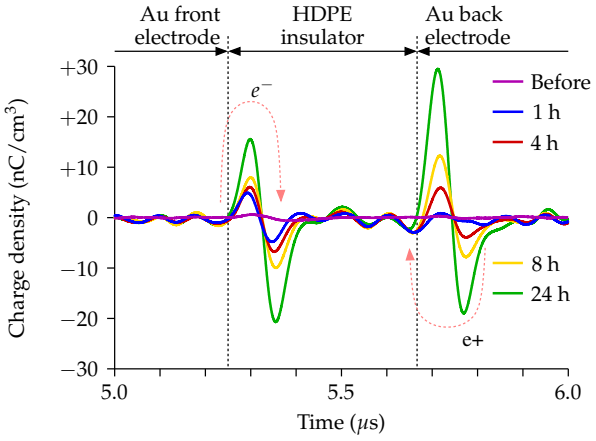

Figure 13: Signals of charge injection in HDPE samples measured under short-circuit for various durations under 40 kV at 22 °C. Samples are coated with gold electrodes, and coupled with 1 mm-thick carbon-loaded polymer (EVA) through silicone oil and tested in the PWP setup. Dotted lines indicate when the pressure pulse begains to cross an interface, the direction of movement of electrons and holes is illustrated by the pink arrow.

When coated with gold electrodes, as shown in Figure 13, charges were clearly injected at both interfaces of the sample and trapped close to the interface without significant diffusion inside the sample. Compared with aluminum coating, gold electrode favors charge injection at the anode and limits charge injection at the cathode. This is totally consistent with the observed interface voltage since the electrode

Fermi level gets farther from the insulator conduction band and closer to the insulator valence band.

As in the case of LDPE, aluminum electrode favored electron injection while gold electrode favored hole injection. However contrarily to LDPE, charges diffused much more less in HDPE than in LDPE as already known [22], the subsequent injection due to heterocharge build-up is thus not observed.

4 Conclusions

HDPE and LDPE samples coated with different types of electrodes were measured under low voltage to determine the interface dipoles leading to interface voltage, and under high voltage to analyze whether these interface voltages have an effect on the charge injection process. A comparison of interface voltage and charge injection under voltage shows that, when coated with aluminum electrodes, the energy levels of HDPE and LDPE are bent downwards, favoring electron injection at the cathode and reducing charge injection at the anode. On the contrary, gold electrodes bend upwards the energy levels of HDPE and LDPE, promoting hole injection at the anode and reducing electron injection at the cathode. The charge buildup under voltage confirms the assumption for both kinds of electrode. Once charges injected in the material, they diffuse more easily in LDPE than in HDPE due to the material conductivity, creating in turn heterocharges that triggered another injection only in LDPE. In conclusion, interface dipoles well explain how charge are injected at first in LDPE and in HDPE. It can be assumed that energy band bending close to the interfaces further reduces the Schottky barrier at that interface compared to the applied electric field solely. The measurement of the interface dipoles to estimate interface voltage could then help to chose materials in contact with insulator subjected to high voltage and to check if two contact conditions could be equivalent or not for tests.

References

[1] K. Chi Kao. *Dielectric phenomena in solids*. Elsevier, 2004.

[2] G. Blaise. Space-charge physics and the breakdown process. *Journal of Applied Physics*, 77(7):2916–2927, April 1995. doi: 10.1063/1.358707.

[3] J. C. Fothergill. Ageing, space charge and nanodielectrics: Ten things we don't know about dielectrics. In *2007 IEEE International Conference on Solid Dielectrics*, pages 1–10, July 2007. doi: 10.1109/ICSD.2007.4290739.

[4] R. Coelho. *Physics of Dielectrics for the Engineer*, volume 1. Elsevier, 2012.

[5] S. M. Sze. *Semiconductor devices: physics and technology*. John wiley & sons, 2008.

[6] C. Kittel. *Introduction to solid state physics*. John Wiley & sons, inc, 2005.

[7] E.H. Nicollian and J.R. Brews. *MOS (Metal Oxide Semiconductor) physics and technology*. John Wiley & Sons, USA, 1982. ISBN: 0471085006.

[8] L. Zheng and S. Holé. Study of contact conditions at conductor/insulator interfaces used in space charge distribution measurements. *Physica Scripta*, 98(2):025802, jan 2023. doi: 10.1088/1402-4896/acad3f.

[9] P. Laurenceau, J. Ball, G. Dreyfus, and J. Lewiner. New principle for the determination of potential distributions in dielectrics. 1976. doi: 10.1103/PhysRevLett.38.46.

[10] B. Salamé and S. Holé. The pressure wave propagation method for the study of interface electric field. In *2015 IEEE Electrical Insulation Conference (EIC)*, pages 53–56, 2015. doi: 10.1109/ICACACT.2014.7223595.

[11] S. Holé, T. Ditchi, and J. Lewiner. Non-destructive methods for space charge distribution measurements: what are the differences? *IEEE Transactions on Dielectrics and Electrical Insulation*, 10(4):670–677, 2003. doi: 10.1109/TDEI.2003.1219652.

[12] J. R. Dennison and Lee H. Pearson. Pulsed electro-acoustic (pea) measurements of embedded charge distributions. In Edward W. Taylor and David A. Cardimona, editors, *Nanophotonics and Macrophotonics for Space Environments VII*. SPIE, September 2013. doi: 10.1117/12.2025667.

[13] G. Rincon, L. Berquez, T. Paillat, and P. LeBlanc. Measurement of the charge distribution at the solid/liquid interface by a new version of the pea method. pages S8–1–1–7, 2023.

[14] G. Chen, M. Hao, Z. Q. Xu, A. Vaughan, J. Cao, and H. Wang. Review of high voltage direct current cables. *CSEE Journal of Power and Energy Systems*, 1(2):9–21, 2015. doi: 10.17775/CSEEJPES.2015.00015.

[15] L. Douminge. *Etude du comportement du polyéthylène haute densité sous irradiation ultraviolette ou sollicitation mécanique par spectroscopie de fluorescence*. Theses, Université de La Rochelle, May 2010.

[16] S. Ronca. Polyethylene. In *Brydson's plastics materials*, pages 247–278. Elsevier, 2017. doi: 10.1016/B978-0-323-35824-8.00010-4.

[17] S. Holé and J. Lewiner. Design and optimization of unipolar pressure pulse generators with a single transducer. *J. Acoust. Soc. Am.*, 104:2790–2797, 1998. doi: 10.1121/1.423863.

[18] A. Ndour, S. Holé, P. Leblanc, and T. Paillat. Direct observation of electric charges at solid/liquid interfaces with the pressure-wave-propagation method. *Journal of Electrostatics*, 109:103527, 2021. doi: 10.1016/j.elstat.2020.103527.

[19] W. K. Chen. *The electrical engineering handbook*. Elsevier, 2004.

[20] S. Holé, T. Ditchi, and J. Lewiner. Influence of divergent electric fields on space-charge distribution measurements by elastic methods. *Physical Review B*, 61(20):13528, 2000. doi: 10.1103/PhysRevB.61.13528.

[21] G. Chen, T.Y.G. Tay, A.E. Davies, Y. Tanaka, and T. Takada. Electrodes and charge injection in low-density polyethylene using the pulsed electroacoustic technique. *IEEE Trans. Dielectr. EI*, 8:867–873, 2001. doi: 10.1109/94.971439.

[22] G. C. Montanari, G. Mazzanti, F. Palmieri, A. Motori, G. Perego, and S. Serra. Space-charge trapping and conduction in ldpe, hdpe and xlpe. *Journal of Physics D: Applied Physics*, 34(18):2902–2911, September 2001. doi: 10.1088/0022-3727/34/18/325.